Chemical Science

ROYAL SOCIETY OF CHEMISTRY

EDGE ARTICLE

View Article Online
View Journal | View Issue

Cite this: *Chem. Sci.*, 2021, **12**, 12092

All publication charges for this article have been paid for by the Royal Society of Chemistry

Received 24th June 2021
Accepted 8th August 2021

DOI: 10.1039/d1sc03447b

rsc.li/chemical-science

Shedding light on predicting and controlling emission chromaticity in multicomponent photoluminescent systems†

J. Price, B. Balónová, B. A. Blight and S. Eisler *

Predictable colour tuning in multicomponent photoluminescent (PL) systems is achieved using mixtures of simultaneously emitting organic molecules. By mitigating the potential for energy transfer through the control of concentration, the resulting emission chromaticity of five dichromic PL systems is approximated as a linear combination of the emitting components and their corresponding brightness (χ_i, ϕ_i, and $I_{ex,i}$). Despite being limited to dilute solutions (10^{-6} M), colour tuning within these systems was controlled by (1) varying the composition of the components and (2) exploiting the differences in the components' excitation intensities at common wavelengths. Using this approach, white light emission (WLE) was realized using a pre-determined mixture of red, green, and blue emitting organic molecules. Based on these results, materials and devices with built-in or programmable emission colour can be achieved, including highly sought-after WLE.

Introduction

Photoluminescence colour-tuning (PLCT) and control of emission chromaticity are critical for the continued development of functional organic and hybrid materials. Molecular systems capable of PLCT are being targeted for applications including lighting and display technologies,[1] sensors,[2,3] inks and encryption,[4–7] and stimuli-responsive smart materials.[8] These systems include but are not limited to mixed-emitting organic polymers,[9] host–guest metal–organic hybrids,[10,11] and simple mixtures of photoluminescent (PL) organic molecules.[12–15] The emission chromaticity of multicomponent PL systems can be tuned by choice of excitation wavelength and varying the composition of each PL emitter.[12,16,17] For example, there have been multiple accounts of multicomponent PLCT being used to achieve highly sought-after white light emission (WLE) by adjusting the composition of each PL component.[1,12,13,15,18] Despite countless examples of multicomponent WLE PL systems, most appear to have arisen through an iterative process of varying the excitation wavelength and composition of RGB emitters as opposed to predicting and programming WLE into systems using the concept of additive colour mixing.

The concept of additive colour-mixing is well established. Combining two or more colours in equal proportion and brightness results in a colour derived from a linear combination of the components.[19] However, many multicomponent PL systems possess intra- or intermolecular energy transfer (ET) mechanisms such as Fluorescence Resonance Energy Transfer (FRET).[11,13,14,20,21] Accounting for ET processes makes applying colour-mixing theory a challenge since ET differs from system to system. However, what if ET processes were mitigated or suppressed? Ingenious strategies to inhibit ET have been explored, including the use of micelles to spatially isolate PL emitters, leading to the simultaneous emission of each component.[14,22] Since ET is distance-dependant, simply controlling the molecular concentration can decrease the possibility of ET, which would allow the resulting emission chromaticity to be approximated as a product of each PL component's emission colour and brightness.

Using the Commission Internationale de l'Eclairage (CIE) 1931 xyz colour-matching functions, the emission spectrum of a PL emitter can be converted into a set of numerical coordinates (x,y) that defines its colour.[19] The brightness (a) of a PL emitter is loosely described as a product of (1) how strongly a PL molecule absorbs light at a given wavelength ($\varepsilon = Acl$) and (2) how much of that absorbed light is subsequently emitted (ϕ_{PL}).[23] Alternatively, one can also describe how strongly a PL molecule absorbs light at a given wavelength by substituting absorption intensity (A) for excitation intensity (I_{ex}). Whereas the absorption intensity is measured as the logarithmic fraction of incident and transmitted light, the signal intensity (counts per second) in the excitation spectrum is directly proportional to the number of photons that are absorbed and emitted. Using excitation intensity (I_{ex}) as a metric to quantify brightness has added benefits such as eliminating the need for a UV-vis spectrophotometer and the advantage of using lower sample concentrations due to the inherent sensitivity of fluorescence spectroscopy. For these reasons, excitation intensity (I_{ex}) can

Department of Chemistry, University of New Brunswick, Fredericton, New Brunswick, E3B 5A3, Canada. E-mail: seisler@unb.ca

† Electronic supplementary information (ESI) available. See DOI: 10.1039/d1sc03447b

serve as a more useful metric for quantifying molecular brightness.

In the absence of ET processes, we propose that the emission chromaticity of a multicomponent PL system can be approximated as a linear combination of each PL component's CIE coordinates (x,y) and their respective contribution *or relative brightness* (a_i) (eqn (1)). Herein, we define each component's contribution *or relative brightness* (a_i) as the product of the ith components mole fraction (χ_i), photoluminescent quantum yield (ϕ_i), and excitation intensity ($I_{ex,i}$) at a common wavelength (eqn (2)).

$$(x_{mix}, y_{mix}) = a_1(x_1, y_1) + a_2(x_2, y_2) + \cdots + a_i(x_i, y_i) \quad (1)$$

$$a_i = \frac{\chi_i \phi_i I_{ex,i}(\lambda_{ex})}{\sum_{i=1}^{n} \chi_i \phi_i I_{ex,i}(\lambda_{ex})} \quad (2)$$

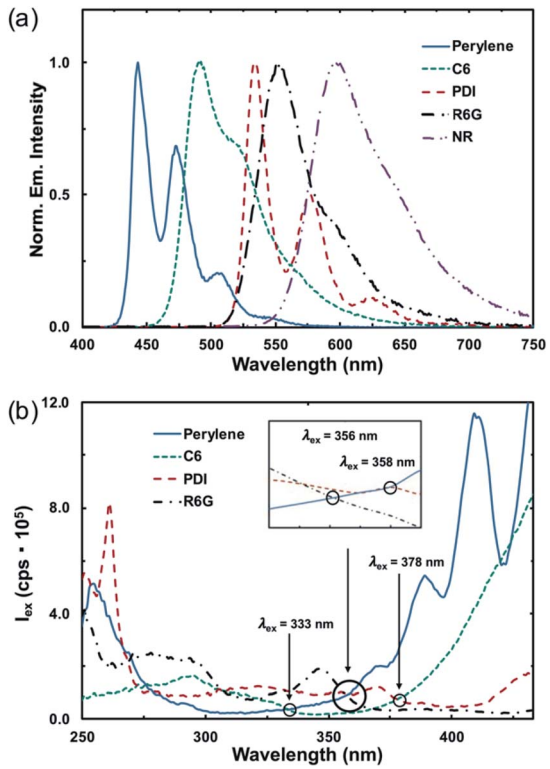

Fig. 1 (a) Overlaid normalized emission profiles of perylene, C6, R6G, PDI, and NR in chloroform. (b) Overlaid excitation profiles of perylene (λ_{em} = 443 nm), C6 (λ_{em} = 491 nm), R6G (λ_{em} = 552 nm), and PDI (λ_{em} = 534 nm) in chloroform ($c = 1.2 \times 10^{-6}$ M). Common excitation wavelengths (λ_{ex}) in which two emitters share similar intensities (I_{ex}) are highlighted.

To test whether the emission chromaticity of a multicomponent PL system can be described as a linear combination of its components, various commercially available PL emitters including perylene, coumarin 6 (C6), *N*,*N*′-bis(3-pentyl)perylene-3,4,9,10-bis(dicarboximide) (PDI), Rhodamine 6G (R6G), and Nile Red (NR) were chosen and subsequently evaluated. Equimolar solutions of each emitter in chloroform ($c = 1.2 \times 10^{-6}$ M) were prepared, and both emission and excitation profiles were obtained at room temperature (Fig. 1a and b; S2–S11, ESI†). The emission maximum (Table 1) of each emitter was identified and then used to record the corresponding emitter's excitation spectrum (p. S3, ESI†).

We then compared each PL components' excitation intensity (I_{ex}) at common wavelengths (Table 1, entries 1–6) within a given system. Consequently, this allowed us to scale each PL component's contribution or relative brightness (eqn (2)) with respect to any excitation wavelength (λ_{ex}) that is used to excite the system. However, for our initial experiments, an excitation wavelength for each system was chosen such that each emitter shared approximately the same excitation intensity (I_{ex})—corresponding to the region where the excitation spectra overlap for each respective system (Fig. 1b). Since the excitation intensities for each component were approximately the same (Table 1, entries 1–5), we expected that any observed difference in emission chromaticity would largely depend on the differences in quantum yields and mole fractions of each PL component.

Two-component PLCT

We subsequently prepared mixtures with varying mole fractions ($\chi_1 : \chi_2$ = 1 : 0, 0.75 : 0.25, 0.50 : 0.50, 0.25 : 0.75, 0 : 1) of five

Table 1 Compiled photophysical data of PL emitters used in this work[a]

					I_{ex} (cps)					
				Entry	1	2	3	4	5	6
PL emitter	λ_{em} (nm)	ϕ_{PL}[b]	CIE (x,y)		λ_{ex} 333 nm	λ_{ex} 347 nm	λ_{ex} 356 nm	λ_{ex} 358 nm	λ_{ex} 378 nm	λ_{ex} 389 nm
Perylene	443	0.92	0.14, 0.09		38 170	40 840	92 770	92 900	—	54 310
C6	491	0.92	0.19, 0.53		35 630	—	—	—	70 342	14 860
PDI	534	0.67	0.37, 0.61		—	—	—	92 670	76 520	—
R6G	552	1	0.42, 0.57		—	—	100 800	—	—	—
NR	597	0.91	0.60, 0.39		—	39 300	—	—	—	—

[a] Reported solution data was measured in aerated chloroform ($c = 1.2 \times 10^{-6}$ M) at room temperature. CIE coordinates (x,y) were extracted from the emission profiles using the Fluoracle® software package. [b] Absolute photoluminescence quantum yields (ϕ_{PL}) were obtained using an Edinburgh FS5 spectrofluorometer equipped with an SC-30 integrating sphere.

different dichromic systems (perylene–C6, perylene–PDI, perylene–R6G, perylene–NR, and PDI–C6) and measured their emission spectra. A total molecular concentration of 1.2×10^{-6} M was chosen to suppress the efficiency of any potential ET processes occurring in solution, such as FRET, which can occur up to 100 angstroms.[24] As a result, the average distance between molecules can be approximated to be greater than 1000 angstroms for our studies (Fig. S1, ESI†). By selecting an excitation wavelength (λ_{ex}) in which each component had similar excitation intensities (I_{ex}), the differences in the measured emission chromaticity were shown to be linearly proportional to the mole fraction (χ) and PLQY (ϕ_{PL}) of each component ($R^2 > 0.98$; Fig. S12–S30, ESI†). The experimentally determined CIE coordinates were then compared to the predicted results obtained using eqn (1) (Tables S1–S7, ESI†). To measure the accuracy of the approximation, absolute errors were quantified based on the distance between the measured and predicted CIE coordinates. For all five dichromic PL systems that were explored in this study, the distance between the measured and predicted CIE coordinates never exceeded 0.02 au, which demonstrates that emission chromaticity within these systems can be accurately described as a linear combination of each PL component (Fig. 2a; Tables S1–S7, ESI†). Based on this result, dichromic PL systems can be used to design emissive materials with any desired chromaticity (x,y), given that it traverses the line between each component by simply adjusting the mole fractions (χ) of the PL components.

A linear relationship between excitation wavelength and the emission CIE coordinates of homometallic Ln(III)-complexes has previously been established.[17] By varying the excitation wavelength, each component's contribution to the overall chromaticity can be controlled due to their differences in excitation intensity. Therefore, we wanted to show that by accounting for the relative differences in excitation intensities of each PL component, the emission chromaticity resulting from excitation at any wavelength can still be approximated as a linear combination of each emitter. To demonstrate this, the mixtures of perylene and C6 that were excited at 333 nm ($I_{ex,perylene} \cong I_{ex,C6}$; Table 1, entry 1), shown in Fig. 2a–c, were excited at 389 nm ($I_{ex,perylene} \neq I_{ex,C6}$; Table 1, entry 6) for comparison.

At $\lambda_{ex} = 333$ nm, perylene and C6 have approximately the same excitation intensities (Table 1, entry 1), and therefore the emission chromaticity is shown to be primarily dependent on the differences in mole fractions and PLQYs of each emitter (Fig. 2a–c, S13 and S14, ESI†). In comparison, when the same mixtures of perylene and C6 are excited at 389 nm, a blue shift is observed in the emission chromaticity that is proportional to the difference in the excitation intensities of perylene and C6 (Table 1, entry 6; Fig. 3a, b and S15, S16, ESI†). Good agreement between the measured and predicted CIE coordinates (abs. error < 0.01 au; Tables S1 and S2, ESI†) was obtained by accounting for the different excitation intensities, mole fractions, and PLQYs of perylene and C6. Based on these results, not only is PLCT possible but any desired emission chromaticity that traverses the 1D-line between two PL components can be targeted by (1) adjusting the mole

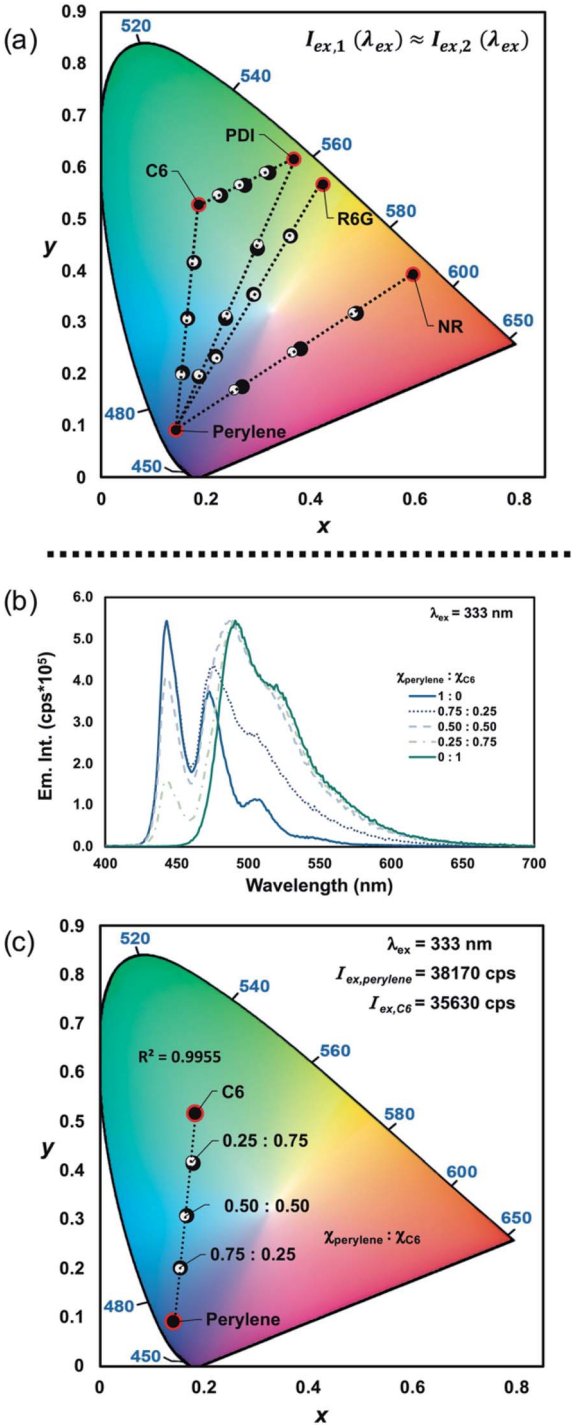

Fig. 2 (a) CIE diagram showing the measured (●) and predicted (○) CIE coordinates obtained from mixtures of perylene–C6 ($\lambda_{ex} = 333$ nm), C6–PDI ($\lambda_{ex} = 378$ nm; $I_{ex,C6} \approx I_{ex,PDI}$), perylene–PDI ($\lambda_{ex} = 358$ nm; $I_{ex,perylene} \approx I_{ex,PDI}$), perylene–R6G ($\lambda_{ex} = 347$ nm; $I_{ex,perylene} \approx I_{ex,R6G}$), and perylene–NR ($\lambda_{ex} = 356$ nm; $I_{ex,perylene} \approx I_{ex,NR}$) with varying mole fractions. (b) Overlaid emission spectra of perylene–C6 ($\lambda_{ex} = 333$ nm; $I_{ex,perylene} \approx I_{ex,C6}$) with varying mole fractions and (c) the corresponding CIE diagram showing the measured (●) and predicted (○) CIE coordinates.

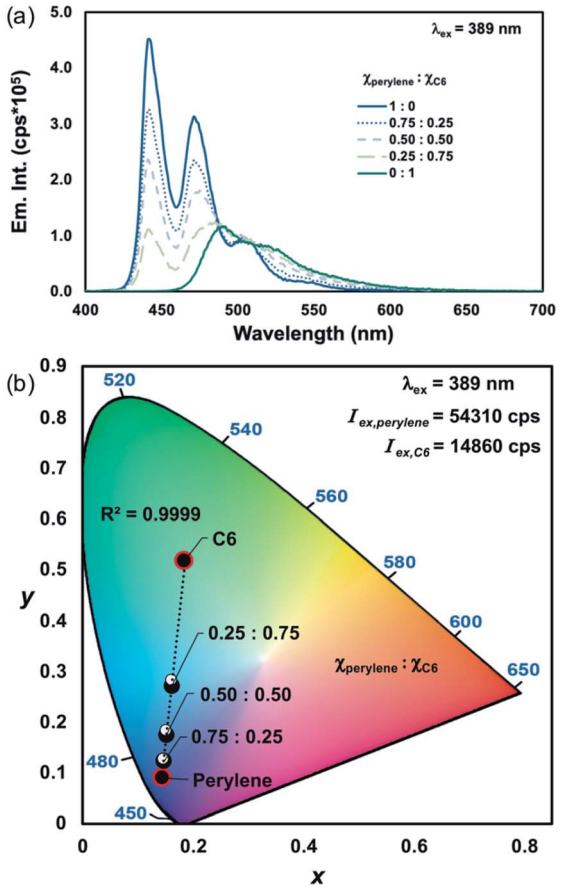

Fig. 3 (a) Perylene–C6 emission profiles (λ_{ex} = 389 nm) with varying mole fractions in chloroform ($c = 1.2 \times 10^{-6}$ M) and (b) the corresponding CIE diagram showing the measured (●) and predicted (○) CIE coordinates.

fractions of the components or (2) strategic selection of an excitation wavelength.

Excitation dependant PLCT

To further illustrate the significance of excitation-based PLCT, while also verifying that the approximation is accurate across a wide range of excitation wavelengths, a mixture of perylene and R6G with equal mole fractions was excited at various wavelengths between 347–367 nm at 2 nm intervals (Fig. 4a–c). Given that there is a suitable overlapping region in the excitation profile of the components, as is the case for perylene and R6G between 347–367 nm (Fig. 4a), emission chromaticity spanning considerable distances can be accessed by merely controlling the excitation wavelength (Fig. 4c). Based solely on the differences in excitation intensities of the emitters at different wavelengths (Table S6, ESI†), the emission is tuned from yellow-green to blue by simply adjusting the excitation wavelength from 347–367 nm at 2 nm intervals (Fig. 4b and c). This result was supported by an observed dependence between the excitation intensities of the components and the resulting emission chromaticity (R^2 = 0.9975; Fig. S27, ESI†). When exciting the perylene–R6G mixture using 347 nm light, R6G's emission is the major contributor primarily due to its larger excitation intensity—conversely, exciting the mixture using 367 nm light results in a chromaticity mainly composed of perylene's blue emission (Fig. 4a). In addition, near-WLE was observed by exciting the perylene–R6G mixture at 355 nm (0.30, 0.37) and 357 nm (0.28, 0.34) (Table S6, ESI†).[26] Good agreement between the measured and predicted CIE coordinates was obtained (Table S6, ESI†). Admittedly, the CIE coordinates appear to deviate from linearity as the excitation wavelength decreased (Fig. 4c). The non-linearity led to an increase in distance between the measured and predicted CIE coordinates (approx.

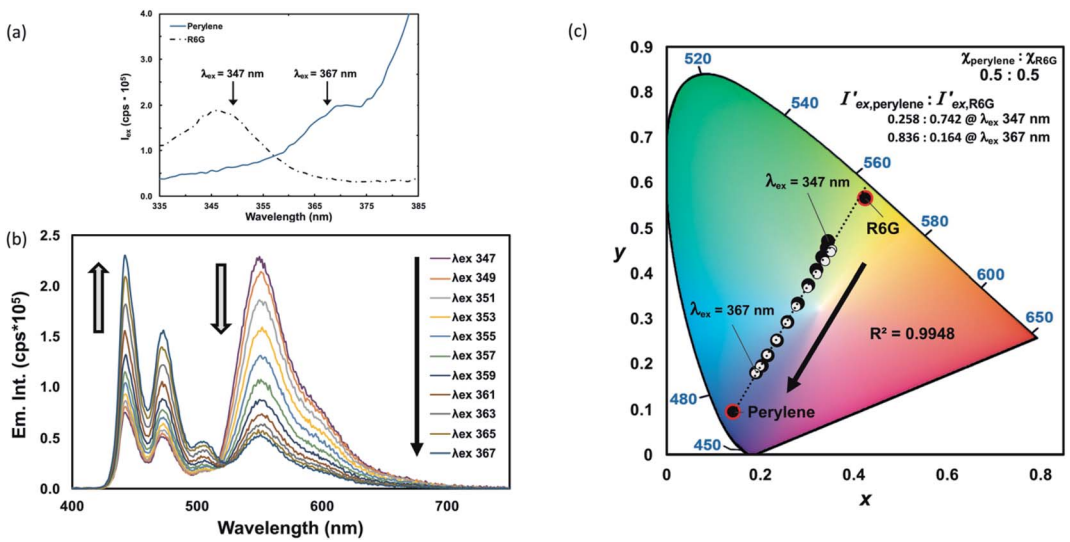

Fig. 4 (a) Overlaid excitation profiles of perylene and R6G in chloroform ($c = 1.2 \times 10^{-6}$ M) showing the region of interest. (b) Perylene–R6G emission profiles in chloroform ($c = 1.2 \times 10^{-6}$ M) obtained at various excitation wavelengths (347–367 nm, 2 nm intervals) and (c) the corresponding CIE diagram showing the measured (●) and predicted (○) CIE coordinates. Relative excitation intensities of perylene $\left(I'_{ex,perylene} = \frac{I_{ex,perylene}}{I_{ex,perylene} + I_{ex,R6G}}\right)$ and R6G $\left(I'_{ex,R6G} = \frac{I_{ex,R6G}}{I_{ex,perylene} + I_{ex,R6G}}\right)$ were calculated using the intensities shown in Table S6, ESI.†

0.02 au; Table S6, ESI†), however, this may be attributed to thermal blooming, a beam-defocusing effect that has been observed when studying R6G.[25]

Three-component PLCT (WLE)

We have demonstrated that in the absence of ET, the emission chromaticity of dichromic PL systems is accurately predicted as a linear combination of its components and their corresponding properties (eqn (1) and eqn (2)). Granted that ET continues to be suppressed, this principle can be applied to systems consisting of any number of PL emitters. As illustrated, dichromic PLCT is limited to colors that traverse the 1D-line connecting the two PL emitters. However, by incorporating three or more PL emitters, a 2D color space or gamut defined by the CIE-coordinates of each PL component is formed (Fig. S34, ESI†). Analogous to dichromic PLCT, access to any chromaticity that resides within the 2D color space is achieved by controlling the contribution or relative brightness (a_i) of each PL component that defines the space—which we have shown is possible by (1) adjusting the composition (χ_i) of each component or (2) varying the excitation wavelength used to excite the system. Using this approach, we aimed to target highly desirable WLE (CIE = 0.33, 0.33) using a pre-determined combination of RGB emitters (perylene, C6, and NR, respectively). Despite there being many examples of mixing three primary or two complementary PL coloured emitters to access WLE, to the best of our knowledge, there has not been an example in which the composition of the RGB emitters that are necessary to achieve WLE is pre-determined based on the properties (χ_i, ϕ_i, and $I_{ex,i}(\lambda_{ex})$) of each emitter.

By treating the ideal WLE coordinates as a barycenter, we calculated the normalized contributions of perylene ($a_1 = 0.34$), C6 ($a_2 = 0.28$), and NR ($a_3 = 0.38$) that are required to achieve WLE (Fig. S34; eqn (S3)–(S7), ESI†). Subsequently, an excitation wavelength was chosen wherein each PL component had comparatively high intensities (λ_{ex} = 274 nm; $I_{ex,perylene}$ = 99 590 cps, $I_{ex,C6}$ = 130 500 cps, and $I_{ex,NR}$ = 137 900 cps; Fig. S35, ESI†). However, it should be noted that any excitation wavelength in which each PL component has a non-zero intensity could have been chosen. Next, we determined the necessary mole fractions of perylene ($\chi_{perylene} = 0.41$), C6 ($\chi_{C6} = 0.26$), and NR ($\chi_{NR} = 0.33$) by selecting an arbitrary concentration of perylene and calculating the corresponding concentrations of C6 and NR needed to satisfy their contribution requirements (p. S28, ESI†). We then acquired the emission spectrum of a mixture of perylene–C6–NR (0.41 : 0.26 : 0.33) in chloroform, and as expected, the mixture's emission spectrum spanned the entire visible region and consisted of each emitter's characteristic emission profile (Fig. 5a). Moreover, the CIE coordinate (0.33,0.34) resulting from exciting the mixture at 274 nm was exceptionally close (<0.01 au) to the ideal WLE coordinate (0.33,0.33) that was targeted (Fig. 5b).

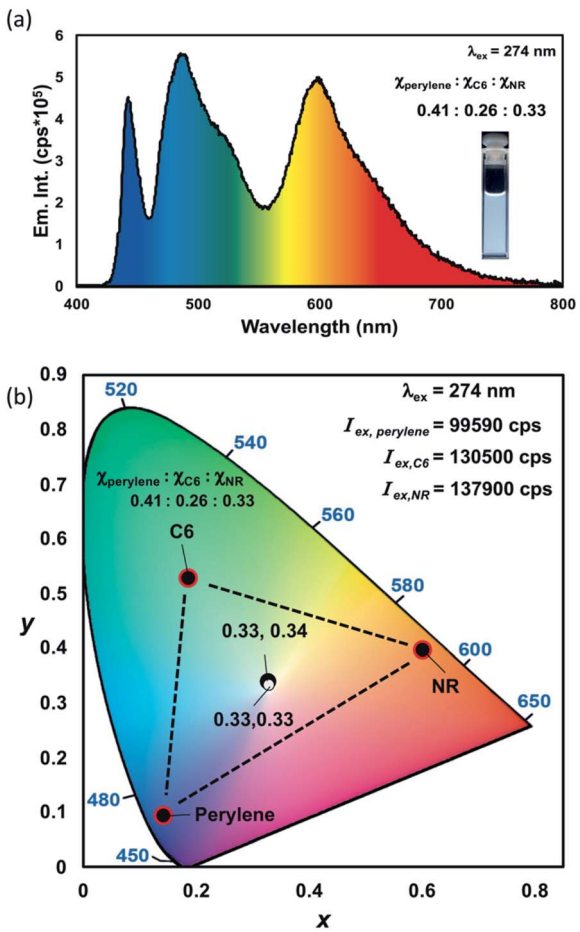

Fig. 5 (a) The emission spectrum (λ_{ex} = 274 nm) of the perylene–C6–NR mixture ($\chi_{perylene} : \chi_{C6} : \chi_{NR}$ = 0.41 : 0.26 : 0.33) in chloroform (c = 1.2 × 10^{-6} M) and (b) the corresponding CIE diagram showing the measured (●) and targeted (○) CIE coordinates. The inset showing the WLE produced by the perylene–C6–NR mixture was irradiated at 365 nm using a TLC lamp.[27]

Conclusion

To summarize, we demonstrated that in the absence of significant ET and quenching processes, the emission chromaticity of a multicomponent PL system can be described as a linear combination of each component's CIE coordinates and corresponding brightness (eqn (1) and (2)). However, until an effective strategy is developed to inhibit ET processes, the accuracy and predictive power of this approach is currently limited to dilute solutions. Predictable PLCT in five dichromic PL systems (perylene–C6, perylene–PDI, perylene–R6G, perylene–NR, and C6–PDI) was shown by adjusting (1) the mole fractions of each component and (2) the excitation wavelength used to excite the system. Linear dependences of χ_i, ϕ_i, and $I_{ex,i}$ with emission chromaticity was established, and good agreement between the measured and predicted CIE coordinates was obtained. This approach was extended to trichromic PL systems wherein we showed that the composition of perylene–C6–NR needed to access WLE could be pre-determined. Using this method, emissive materials with any desired emission colour can be targeted by strategically combining PL emitters. In addition, devices with programmable PL colour are achievable using

excitation wavelength as an input to control the resulting colour.

Data availability

All experimental details supporting this article are provided in the ESI.†

Author contributions

J. P. conceived the idea and prepared the manuscript. J. P. and B. B. performed all experiments and investigations. S. E. and B. A. B. co-supervised this work. B. A. B. provided the instrumentation required for the measurements. S. E. acquired the financial support and resources for the project. All authors discussed the results, provided scientific input, and peer-reviewed the manuscript.

Conflicts of interest

There are no conflicts to declare.

Acknowledgements

All authors thank Natural Sciences and Engineering Research Council of Canada (NSERC - RGPIN-2017-04462) and the New Brunswick Innovation Foundation (RIF 2018-034) for support of this work.

References

1 M. Pan, W.-M. Liao, S.-Y. Yin, S.-S. Sun and C.-Y. Su, *Chem. Rev.*, 2018, **118**, 8889–8935.
2 K. Müller-Buschbaum, F. Beuerle and C. Feldmann, *Microporous Mesoporous Mater.*, 2015, **216**, 171–199.
3 H. Ding, S.-B. Yu, J.-S. Wei and H.-M. Xiong, *ACS Nano*, 2016, **10**, 484–491.
4 Q. Wang, Q. Zhang, Q.-W. Zhang, X. Li, C.-X. Zhao, T.-Y. Xu, D.-H. Qu and H. Tian, *Nat. Commun.*, 2020, **11**, 158.
5 C. N. Zhu, T. Bai, H. Wang, W. Bai, J. Ling, J. Z. Sun, F. Huang, Z. L. Wu and Q. Zheng, *ACS Appl. Mater. Interfaces*, 2018, **10**, 39343–39352.
6 X. Hou, C. Ke, C. J. Bruns, P. R. McGonigal, R. B. Pettman and J. F. Stoddart, *Nat. Commun.*, 2015, **6**, 6884.
7 M. Zuo, W. Qian, T. Li, X.-Y. Hu, J. Jiang and L. Wang, *ACS Appl. Mater. Interfaces*, 2018, **10**, 39214–39221.
8 X. Ji, W. Chen, L. Long, F. Huang and J. L. Sessler, *Chem. Sci.*, 2018, **9**, 7746–7752.
9 K. Wei, G. Wen, Y. Zhao, Z. Lin, X. Mei, L. Huang and Q. Ling, *J. Mater. Chem. C*, 2016, **4**, 9804–9812.
10 B. Balónová, D. R. Martir, E. R. Clark, H. J. Shepherd, E. Zysman-Colman and B. A. Blight, *Inorg. Chem.*, 2018, **57**, 8581–8587.
11 T. Ono and Y. Hisaeda, *J. Mater. Chem. C*, 2019, **7**, 2829–2842.
12 N. Muhamad Sarih, P. Myers, A. Slater, B. Slater, Z. Abdullah, H. A. Tajuddin and S. Maher, *Sci. Rep.*, 2019, **9**, 11834.
13 Y. I. Park, O. Postupna, A. Zhugayevych, H. Shin, Y.-S. Park, B. Kim, H.-J. Yen, P. Cheruku, J. S. Martinez, J. W. Park, S. Tretiak and H.-L. Wang, *Chem. Sci.*, 2015, **6**, 789–797.
14 R. Wang, J. Peng, F. Qiu and Y. Yang, *Chem. Commun.*, 2011, **47**, 2787–2789.
15 B. Kumari, M. Paramasivam, A. Dutta and S. Kanvah, *ACS Omega*, 2018, **3**, 17376–17385.
16 R. L. Ayscue, C. P. Verwiel, J. A. Bertke and K. E. Knope, *Inorg. Chem.*, 2020, **59**, 7539–7552.
17 W.-M. Liao, C.-J. Li, X. Wu, J.-H. Zhang, Z. Wang, H.-P. Wang, Y.-N. Fan, M. Pan and C.-Y. Su, *J. Mater. Chem. C*, 2018, **6**, 3254–3259.
18 W. Wang, R. Wang, Y. Ge and B. Wu, *RSC Adv.*, 2018, **8**, 42100–42108.
19 J. Schanda, *Colorimetry: understanding the CIE system*, John Wiley & Sons, Inc., Hoboken, N.J, 2007.
20 B. Manna, A. Nandi and R. Ghosh, *Photochem. Photobiol. Sci.*, 2019, **18**, 2748–2758.
21 M. Nara, R. Orita, R. Ishige and S. Ando, *ACS Omega*, 2020, **5**, 14831–14841.
22 J. Peng, M. Chen, F. Qiu, Y. Yang, B.-H. Sohn and D. H. Kim, *Appl. Phys. Lett.*, 2008, **93**, 183303.
23 K. D. Piatkevich and V. V. Verkhusha, *Methods Cell Biol.*, 2011, **102**, 431–461.
24 S. A. Hussain, arXiv:0908.1815, 2019.
25 A. M. Brouwer, *Pure Appl. Chem.*, 2011, **83**, 2213–2228.
26 Note that in the case of perylene and R6G, the line connecting the two emitters never actually crosses pure WLE (0.33,0.33). However, one could calculate the coordinate on the line that is nearest to 0.33,0.33, choose an excitation wavelength where each component has a suitable intensity, and then calculate the ratio of emitters that are needed to achieve the CIE coordinate closest to WLE.
27 CIE diagrams were adapted from Wikimedia Commons, "CIE 1931 Chromaticity Diagram.jpg" by Magica, licensed under CC BY-SA 4.0/ modified border (https://creativecommons.org/licenses/by-sa/4.0/).